Pergamon

SCIENCE DIRECT®

Bioorganic & Medicinal Chemistry 11 (2003) 811–816

BIOORGANIC & MEDICINAL CHEMISTRY

# A Biaryl Peptide Crosslink in a MetJ Peptide Model Confers Cooperative, Nonspecific Binding to DNA that Ablates Both Repressor Binding and In Vitro Transcription

Joshua C. Yoburn,[a,†] Sipra Deb,[b,†] Iain W. Manfield,[b] Peter G. Stockley[b] and David L. Van Vranken[a,*]

[a]*Department of Chemistry, University of California, Irvine, CA 92697-2025, USA*
[b]*Astbury Centre for Structural Molecular Biology, School of Biochemistry and Molecular Biology, University of Leeds, Leeds, LS2 9JT, UK*

Received 29 August 2002; revised 5 November 2002; accepted 14 November 2002

**Abstract**—The MetJ repressor is the archetypal example of the β-ribbon-helix-helix DNA binding motif. A model of the MetJ β-ribbon (residues 22–28) was prepared by forming a dityrosine crosslinked dimer from the heptapeptide KKYTVSI. Using SPR, the peptide dimer **2** was shown to bind to dsDNA under physiologically relevant conditions, whereas the monomeric peptide did not. The peptide dimer appeared to inhibit binding of the MetJ repressor to natural *met* operators. Based on the stoichiometry of binding, the binding of peptide dimer **2** seems both highly co-operative and to lack sequence specificity. Peptide binding also appears to prevent transcription in vitro.


All living organisms possess critical regulatory proteins that bind to specific DNA sequences. In the majority of cases, these proteins use α-helices to probe the information-rich major groove of DNA. Relative to α-helix/major groove interactions there are far fewer examples of β-ribbon/major groove interactions.[1,2] Some of the currently known examples of β-ribbon DNA binders include the Arc and Mnt repressors from the *Salmonella* bacteriophage P22, TraY, CopG and NikR proteins also belong to this class.[3–8]

Arc repressor grips DNA with nanomolar affinity by wedging two identical $C_2$ symmetric antiparallel β-ribbons into the major groove. Helbecque and co-workers synthesized a β-hairpin peptide inspired by Arc repressor β-ribbons but lacking the tryptophan residues and local $C_2$ symmetry of the natural system.[9] The Arc β-hairpin peptide bound to the Arc operon with modest affinity ($K_D$ 87 μM) whereas a peptide corresponding to a single strand of the Arc β-ribbon did not exhibit measurable affinity for DNA.

MetJ is the structural archetype of the β-ribbon-helix-helix class of DNA binding proteins.[10,11] The high affinity and specificity of MetJ for DNA is achieved, at least in part, using a single β-ribbon motif (Fig. 1). The $C_2$ symmetry of the MetJ homodimer leads to selectivity for the palindromic consensus sequence AGACGTCT (the met box).[12,13] Two elegant β-ribbon models of MetJ have been prepared previously. The first model, made by Nambiar and co-workers, was composed of

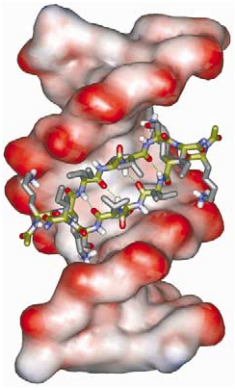

**Figure 1.** (a) Residues 22–28 in the MetJ/DNA complex (1CMA.pdb).

*Corresponding author. Tel.: +1-9498245455; fax: +1-9498248571; e-mail: dlvanvra@uci.edu
†These authors contributed equally to this report.

0968-0896/03/$ - see front matter © 2003 Elsevier Science Ltd. All rights reserved.
PII: S0968-0896(02)00583-7

two identical peptides bridged in the middle by a non-natural disulfide crosslink.[14] The second model, made by Searle and co-workers, consisted of a single peptide chain composed of two MetJ sequences concatenated by an Asn–Gly linker.[15,16] For both models, there is convincing evidence of antiparallel β-structure in solution, but the interactions with DNA have not been assessed. We set out to create a $C_2$ symmetric model of the MetJ β-ribbon, linked by robust carbon–carbon bonds, and study its interaction with DNA.

## Results

### Synthesis of dityrosine peptide dimer 2

The dityrosine-linked model of MetJ was prepared using peroxidase catalysis. Peroxidase-catalyzed dityrosine formation is efficient with the free amino acid but not when tyrosine is incorporated into short peptides.[17] The dityrosine linked peptide dimer **2** was synthesized using a peroxidase catalyzed coupling reaction in 1 M borate buffer at pH 9 (Fig. 2). The reaction was carried out at 5 mM substrate at 37 °C. The dityrosine dimer **2** further undergoes a variety of reactions that compete with the transformation of starting material to dimer. Thus, the reaction must be quenched and purified prior to the full consumption of starting material and dimer in order to achieve an optimal yield. A reaction time of 1 h represented the optimal balance between under-reaction and overreaction (Fig. 3).

Peptide dimer **2** was purified by reverse-phase HPLC (Fig. 4) and its identity confirmed by electrospray mass spectrometry and NMR. While the yield for the dimerization reaction was only 8%, this is higher than any previously reported chemical yield for a peroxidase-catalyzed dimerization of a tyrosine-containing peptide.

### 2D NMR

Dimer **2** was studied by 2D $^1$H NMR in aqueous methanol. The only strong ROESY signals that were observed between vicinal protons. There were no signals suggestive of β-ribbon-type pre-organization as judged by the absence of key long-distance NOE's. Similarly, $H_\alpha$ chemical shift index data is consistent with a random coil in aqueous methanol.

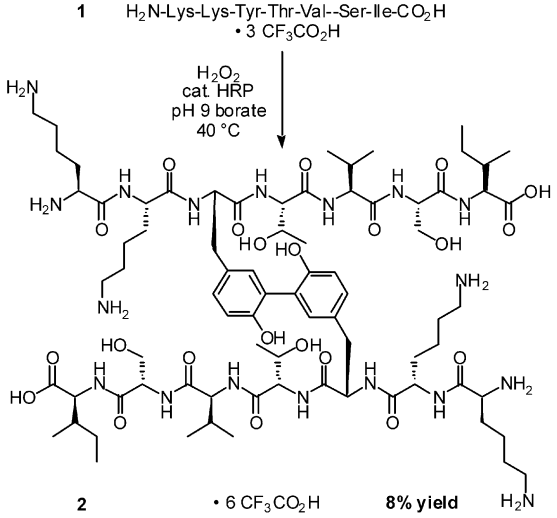


**Figure 2.** Oxidative phenolic coupling of monomer provides dimer.

### SPR Studies

The binding of purified MetJ repressor at differing concentrations to three immobilised DNA fragments encompassing the natural *met* operators, *metC*, *metA* and *metF* was observed (Fig. 5). As expected, the repressor showed binding to all three fragments, the level of apparent saturation being higher for the *metA* and *metF* targets reflecting the larger numbers of met boxes, and hence higher repressor:operator stoichiometries, compared to *metC*.

The peptides **1** and **2** were then dissolved in AB and a concentration series, calculated with respect to monomer, serially injected over the immobilised templates. The results are shown in Figure 5, panel b. Under the conditions used it appeared that peptide **1** did not bind to any of the targets. In sharp contrast, peptide **2** showed rapid high level binding to all three DNA targets. The RU responses are proportional to the amount of mass being immobilised (1000 RU≈1 ng/mm$^2$, the area of each flow-cell being ≈1 mm$^2$). Remarkably, the dimer peptide binding saturates at significantly higher levels than the natural protein ligand, even though its relative molecular mass is ∼14× smaller than the active MetJ dimer. Binding of the peptide is greater to the longer DNA fragment. These results imply that the peptide binds with high stoichiometry with approximately one dimer peptide per 2 bp of duplex target. Presumably, the bulk of this binding is non-sequence

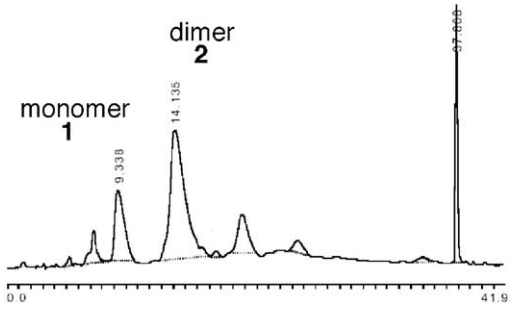


**Figure 3.** HPLC chromatogram of the dimerization reaction after 1 h. 20–35% MeCN/aq 0.1% TFA over 30 min; 35–100% over 5 min.

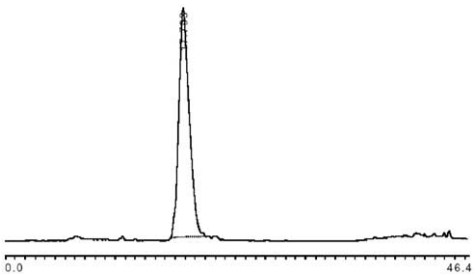


**Figure 4.** HPLC chromatogram of purified dimer. 0–20% MeCN/aq 0.1% TFA over 5 min; 20–35% over 30 min, 35–100% over 10 min.

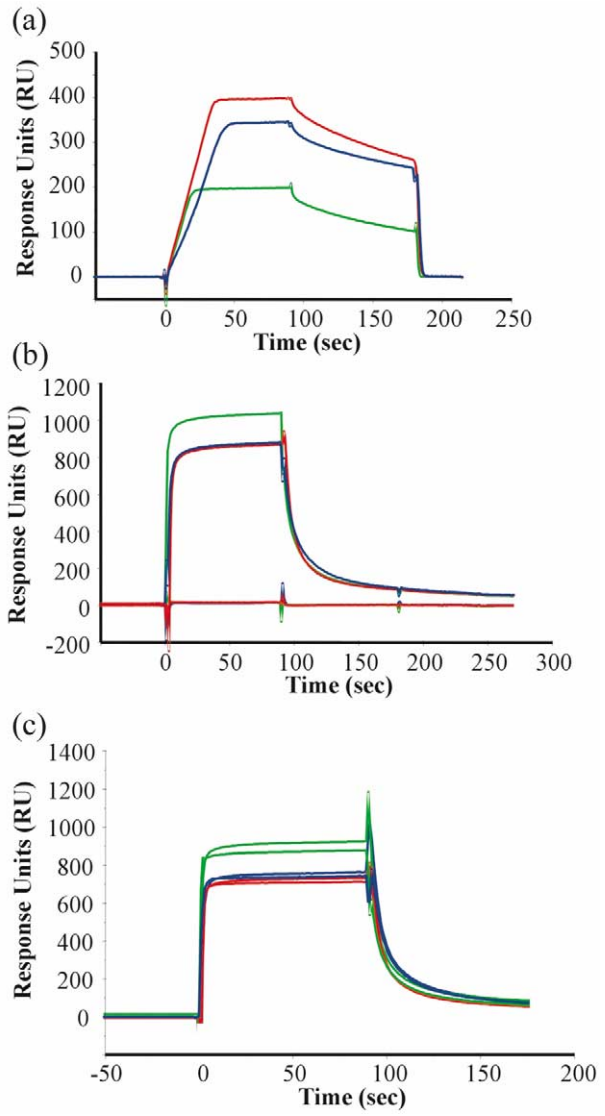


**Figure 5.** (a) MetJ repressor binding to natural *met* operators. MetJ (96 nM dimer, final concentration) was resuspended in AB containing 1mM AdoMet (step 1) and injected across flow cells containing immobilised *metC* (green), *metA* (blue) and *metF* (red) for 90 s. This was followed by a second injection of 1 mM AdoMet in AB alone for another 90 s to observe the dissociation of the holo-repressor complex (step 2). (b) Binding of peptides **1** (below 200 RU) and **2** (above 600 RU) to natural *met* operators. Solutions of peptide **1** and peptide **2** were prepared in AB (final concentrations of 2 and 1 mM, respectively) in the presence of 1 mM AdoMet and injected as for MetJ in (a). (c) Binding of peptide **2** in the presence and absence of MetJ to *met* operators. An injection of peptide **2,** with and without MetJ (1 and 20 nM final concentrations, respectively) in the presence of 1 mM AdoMet in AB was carried out as described in (a and b) above.

specific. The lack of binding selectivity is offset by the strength of the surface-based assay; at high concentrations oligolysines can lead to DNA precipitation through charge neutralization.

Binding of the dimer **2** was essentially undetectable at concentrations $\leq$0.1 mM and was close to saturation at 1 mM, implying that binding was cooperative. The kinetics of the interaction also differ from those seen with the natural protein ligand. MetJ binds with an association rate constant approaching that of a diffusion-limited reaction, as expected for a transcriptional regulatory protein. Binding of the peptide dimer **2** is even more rapid, presumably reflecting its lower molecular weight. We then assessed what would happen if both peptide **2** and MetJ/AdoMet were injected across the targets at the same time. The results are shown in Figure 5, panel C. The kinetics of binding and the levels of saturation reached during the interaction leave little doubt that peptide **2** binding is the dominant event taking place, i.e., peptide **2** ablates the repressor–DNA interaction.

Although the data described above suggest that peptide **2** binds non-sequence specifically, they do not address whether the initial binding is nucleated at met box sites and then peptide–peptide cooperativity allows target saturation. Natural DNA-binding proteins often show such behaviour in vitro. To examine this possibility, we then studied binding to two fragments lacking met box sites, 5S and ABRE (Fig. 6). Binding to these two sites is very similar to binding to the *metC* operator fragment used previously with saturation levels roughly reflecting fragment length.

In vitro transcription of the 5S template and the *metC* fragment on the sensorchip was then studied by injecting T7 RNA polymerase and NTPs (Fig. 6, panel b). The *metC* fragment lacks a T7 promoter and showed no binding, whereas as expected there was an increase in RU during the injection over the 5S template. This was followed by a slow decrease when the injection was terminated due to dissociation of transcript and T7 RNAP. Repeating these injections in the presence of dimer peptide **2** showed binding consistent with peptide binding and dissociation on both templates. The rapid decrease in RU signal when AB was restored to the sensor surface clearly shows that no transcription was possible in the presence of peptide dimer **2**.

## Discussion

Transcriptional control is essential in all living organisms. Proteins are ideally suited for this task, but until recently, there were no examples of transcriptional control using small molecules.[18,19] Ideally, a small $C_2$-symmetric peptide dimer, based on the MetJ β-ribbon, could mimic or inhibit the repressor function of MetJ. Recently, ditryptophan crosslinks have been shown to reinforce antiparallel β-ribbon structure in $C_2$ symmetric peptide dimers.[20] A key advantage of ditryptophan crosslinks over disulfides is that that they are resistant to reductive cleavage. Unfortunately, ditryptophan crosslinks can only connect tryptophan sidechains directly across from each other in antiparallel β-strands (Fig. 7). If a peptide dimer were created from the MetJ(22–28) sequence KKITVSI through a T25W mutation, the ditryptophan would lie on the side of the β-sheet that faces the DNA bases. Dityrosines are close relatives of ditryptophans, but span longer distances. In the minimium energy *R* and *S* biaryl conformations of dityrosine the β-carbons are 8.5 Å apart—an ideal fit for a β-ribbon. Dityrosines should be ideal for joining anti-

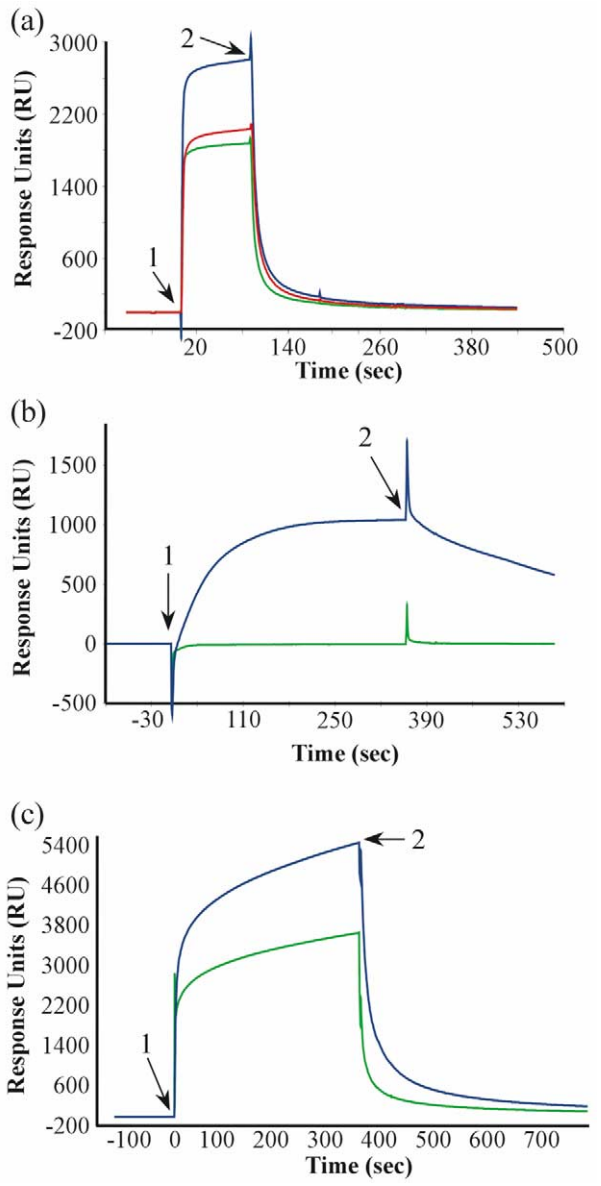


**Figure 6.** 5S (226 bp, 1060 RU), ABRE (226 bp, 775 RU) and *metC* (215 bp, 915 RU) were immobilised as described previously. (a) Peptide 2, at a final concentration of 1 mM in AB containing 1 mM AdoMet, was injected over the targets at a flow rate of 30 μL/min for 90 s at 25 °C. (b) To investigate whether the dimer might have an effect on transcription, a transcription mix containing T7 RNA polymerase (50 nM) and 4 NTP's in transcription buffer, TB (10 mm Tris. HCl pH 7.4, 50 mM NaCl, 4 mm $MgCl_2$, 1 mm DTT, 0.005%(v/v) P20) was injected across the 5S and *metC* targets for 360 s (step 1). Transcription was observed in the form of increasing RU on the 5S template (—) and by the slow dissociation behaviour at the end of the injection (step 2). As expected there was no apparent transcription on the *metC* target (—). (c) The injection described in (b) was repeated in the presence of peptide **2** (final concentration 1 mM) [panel c, colours as in (a and b)].

parallel β-strands through diagonally disposed side-chains (Fig. 7). In this case, a dityrosine crosslink should be able to occupy the face of the β-ribbon opposite the DNA.

The SPR results show that peptide dimer **2** binds to DNA with higher affinity than the monomer, even when normalized for the number of peptide chains. These results are entirely consistent with the well established

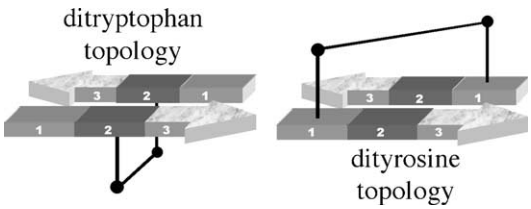


**Figure 7.** Ditryptophan crosslinks and dityrosine crosslinks have complementary topology.

principle of multivalency, but it is important not to take the effect for granted. Multivalency rewards the correct placement of functional groups but also punishes their incorrect placement. The magnitude of these effects is diminished by flexibility.

Without a dimerization domain, the basic region of the bZIP protein GCN4 (222–252) binds poorly to DNA under physiological conditions.[21] However, a simple disulfide crosslink has been shown to restore DNA binding to short pairs of peptides derived from the GCN4 basic region. The DNA sequence specificity of disulfide-linked GCN4 models is retained with peptides as short as 20 amino acids.[22,23] Wadhwa and coworkers have probed the effect of peptide dimerization on the DNA binding ability of oligolysines using peptides with the sequence $[CysTrp(Lys)_n]_2$.[24] For $n = 3$, 8, 13, and 18, disulfide-linked dimers bound to DNA with higher affinity than the corresponding monomers. However, if the results are normalized for the number of peptide chains, dimerization does not provide any benefit over doubling the concentration of the peptide monomer. In this context, it is easier to appreciate the enhanced affinity of the MetJ model **2** relative to the monomer.

On the other hand, the binding of dimer **2** to DNA in some ways resembles the binding of polylysine to oligonucleotides. For example, in the case of oligolysine–DNA interactions, longer oligomers bind more tightly than short oligomers.[25] In addition, biphasic melting curves suggest that oligolysines with eight or more residues bind cooperatively to DNA, however the effect was not observed with tetralysine.[26]

In the crystal structure of the MetJ-DNA complex the β-ribbon covers eight base pairs. The fact that peptide dimer **2** binds to oligonucleotides with a 1:2 (peptide dimer/bp) stoichiometry is consistent with non-selective binding and militates against a model in which dimer **2** binds exclusively in the major groove like the MetJ β-ribbon. Similarly, ROESY data provided no additional NOE evidence indicative of beta structure. However, these results do not preclude the possibility that dimer **2** adopts a well-defined conformation *upon binding* in solution.[27–29]

## Conclusion

These studies demonstrate that a small dimeric peptide model of the MetJ DNA binding region (22–28) can bind to DNA under physiologically relevant conditions. In so doing the peptide dimer **2** inhibits the binding of

the MetJ repressor to natural *met* operators. In contrast, control experiments with the corresponding monomeric peptide **1** (normalized for the number of peptide chains) did not reveal any DNA binding. Unfortunately the MetJ model **2** did not exhibit sequence specificity, although it was able to ablate in vitro transcription. While two-dimensional NMR revealed no pre-organization of the peptide in solution, the results obtained in binding studies are promising given the simplicity of the model.

Future efforts will be directed towards designing potent and sequence-specific inhibitors of both methionine repressor binding and transcription, as well as investigating the properties of the peptide–DNA complexes formed. This system has potential as a means of targeting specific gene expression and could also be used to template the alignment of molecules along polynucleotide chains.

## Experimental

### General

Amino acids and coupling agents were purchased from NovaBiochem. Analytical and preparative HPLC were carried out using Rainin $C_{18}$ Microsorb stationary phase with a UV detector (254 nm).

**Solid-phase peptide synthesis of peptide 1.** Peptide **1** was prepared on 2.5 g of Fmoc-Ile-Wang resin by manual solid-phase peptide synthesis using HBTU. Amide coupling reactions were judged to be complete using the Kaiser test. The peptide was cleaved from resin using TFA/TIS/$H_2O$ (95:2.5:2.5) over 2 h. The crude peptide was precipitated with ether and purified in 40 mg batches by reversed-phase HPLC on a $C_{18}$ Microsorb using 15–40% acetonitrile/0.1% aq TFA over 30 min. The monomeric peptide **1** was isolated in overall 48% yield. $^1$H NMR (DMSO-$d_6$, 500 MHz, 298 K) δ 9.18 (br s, 1H), 8.52 (d, 1H, $J$ = 7.3 Hz), 8.14 (br s, 1H), 8.09 (d, 1H, $J$ = 7.8 Hz), 8.01 (d, 1H, $J$ = 7.9 Hz), 7.81 (d, 1H, $J$ = 7.8 Hz), 7.72 (br s, 1H), 7.65 (d, 1H, $J$ = 8.7 Hz), 7.04 (d, 2H, $J$ = 8.4 Hz), 6.61 (d, 2H, $J$ = 8.4 Hz), 5.00 (br s, 1H), 4.90 (br s, 1H), 4.56 (ddd, 1H, $J$ = 4.1 Hz, 8.9 Hz, 8.9 Hz), 4.38 (dd, 1H, $J$ = 6.3 Hz, 13.1 Hz), 4.31–4.29 (m, 3H), 4.18 (dd, 1H, $J$ = 6.1 Hz, 12.4 Hz), 4.03 (m, 1H), 3.75 (dd, 1H, $J$ = 6.5 Hz, 6.5 Hz), 3.56 (m, 2H), 2.95 (d, 1H, $J$ = 10.4 Hz), 2.75–2.63 (m, 4H), 2.01 (ddd, 1H, $J$ = 7.0 Hz, 13.3 Hz, 13.3 Hz), 1.76 (m, 1H), 1.64 (m, 3H), 1.50 (m, 6H), 1.38 (m, 1H), 1.30–1.20 (m, 4H), 1.13 (m, 1H), 1.01 (d, 3H, $J$ = 6.4 Hz), 0.87 (d, 3H, $J$ = 6.7 Hz), 0.84–0.81 (m, 11H). HRMS calcd for $C_{39}H_{68}N_9O_{11}$ 838.5038; found 838.5033.

**Synthesis of dityrosine peptide dimer 2.** To a solution of peptide **1** (0.205 g, 5 mM) in 1 M pH 9 borate buffer (20 mL) at 40 °C was added 1 mg horseradish peroxidase (269 U/mg, RZ = 3.0; Sigma) followed by 98 μL of 3% $H_2O_2$. The dityrosine peptide dimer is subject to further oxidative processes and was quenched with 12 μL β-mercaptoethanol before all of the starting material was consumed (1 h). The reaction was lyophilized to give a large quantity of borate salts. The salts were taken up in 10 mL of DI water and the slurry was dialyzed against 1 L water using cellulose ester dialysis tubing (100 MWCO). The dialysis sample was lyophilized to afford 200 mg of crude reaction product which was subjected to reverse phase HPLC purification in 20 mg batches using 20–30% acetonitrile/0.1% aq TFA over 30 min. The dityrosine peptide dimer **2** (16 mg) was isolated as the trifluoroacetate salt in 8% yield. $^1$H NMR ($D_2O/CD_3OD$ 4:1, 500 MHz, 292 K) δ 7.15 (s, 2H, $Tyr_\delta$), 7.08 (d, 2H, $J$ = 7.4 Hz, $Tyr_\delta$), 6.87 (d, 2H, $J$ = 7.4 Hz, $Tyr_\varepsilon$), 5.06 (m, 2H, $Tyr_\alpha$), 4.63 (m, 2H, $Ser_\alpha$), 4.54–4.49 (m, 4H, $Lys_\alpha$), 4.36 (m, 2H, $Thr_\alpha$), 4.12 (d, 2H, $J$ = 6.3 Hz, $Val_\alpha$), 4.09 (d, 2H, $J$ = 6.0 Hz, $Ile_\alpha$), 3.96 (m, 2H, $Thr_\beta$), 3.80 (m, 4H, $Ser_\beta$), 3.17 (t, 2H, $J$ = 4.9 Hz, $Tyr_\beta$), 3.09–2.9 (m, 10H, $Tyr_\beta + Lys_\varepsilon$), 1.92–1.63 (m, 20H, $Lys_\beta + Lys_\delta + Val_\beta + Ile_\beta$), 1.48–1.32 (m, 14H, $Lys_\gamma + Thr_\gamma$), 1.19 (m, 4H, $Ile_\gamma$), 1.08 (d, 6H, $J$ = 5.2 Hz, $Thr_\gamma$), 0.91 (d, 6H, $J$ = 9.0 Hz), 0.88–0.8 (m, 18H, $Val_{\gamma+Ile\delta}$). ESI-MS [M + H] $C_{78}H_{133}N_{18}O_{22}$: 1673.98.

### NMR studies

$^1$H, COSY, ROESY (200 ms mixing time) experiments were performed on a Bruker GN500 spectrometer on 5 mM peptide samples in $D_2O/CD_3OD$ (4:1) or DMSO-$d_6$. All chemical shifts are internally referenced to trimethylsilane (TMS).

### SPR studies

The peptides (both monomer and dimer) were dissolved in analysis buffer (AB; 20 mM Tris. HCl, pH 7.4, 200 mM NaCl, 1 mM EDTA, 0.005% (v/v) P20). DNA fragments that contained varying numbers of natural met boxes (encompassing the natural operators *metC*, *metA* and *metF*, containing 2, 4 and 5 met boxes, respectively) were generated as described previously using the polymerase chain reaction and an appropriately biotinylated primer.[30,31] These were then immobilised on separate flow cells of a streptavidin-coated sensor chip. Approximately 400 response units (RU) worth of each template were immobilised. Binding with purified MetJ repressor was monitored in the presence of 1 mM *S*-adenosylmethionine (AdoMet) as described. A similar amount of AdoMet was added to the peptide reactions, for ease of comparison. A concentration series of both the monomer and dimer peptides (0 mM, 0.1, 0.2, 0.3, 0.4, 0.5 and 1 mM) were each made up in 100 μL of AB. These concentrations of peptide were then serially injected over the immobilised templates at a flow-rate of 30 μL/min, 25 °C and the binding observed. Sensorgrams were corrected for non-specific binding by subtracting traces obtained on adjacent underivatised flow-cells.

As a test of sequence specificity, binding was also assessed against two DNA fragments lacking met box sequences but containing eukaryotic sequences, either from the Xenopus 5S rRNA gene (5S template) or the tobacco abscisic acid response element (ABRE). The 5S template also contained a promoter for the T7 bacter-

iophage RNA polymerase, allowing in vitro transcription on the sensorchip to be analysed. Buffer flow-rates were reduced to 10 μL/min for the transcription reactions.

## Acknowledgements

The work in Leeds was supported by the UK BBSRC. Work within the Astbury Centre is in part supported by the North of England Structural Biology Centre (NESBiC). The work in Irvine was supported by the National Institutes of Health (GM54523).

## References and Notes

1. Kim, S. H. *Science* **1992**, *255*, 1217.
2. Phillips, S. E. V. *Curr. Opinion Struct. Biol.* **1991**, *1*, 89.
3. Bowie, J. U.; Sauer, R. T. *J. Mol. Biol.* **1990**, *211*, 5.
4. Brown, B. M.; Bowie, J. U.; Sauer, R. T. *Biochemistry* **1990**, *29*, 11189.
5. Breg, J. N.; van Ophersden, H. J.; Burgering, M. J. M.; Boelens, R.; Kaptein, R. *Nature* **1990**, *346*, 586.
6. Raumann, B. E.; Brown, B. M.; Sauer, R. T. *Curr. Opinion Struct. Biol.* **1994**, *4*, 36.
7. Gomis-Rüth, F. X.; Sola, M.; Acebo, P.; Parraga, A.; Guasch, A.; Eritja, R.; Gonzalez, A.; Espinosa, M.; del Solar, G.; Coll, M. *EMBO J.* **1998**, *17*, 7404.
8. Chivers, P. T.; Sauer, R. T. *Protein Sci.* **1999**, *8*, 2494.
9. Helbecque, N.; Boutaher, A. E. I.; Henichart, J. P. *Peptide Res.* **1996**, *9*, 21.
10. Rafferty, J. B.; Somers, W. S.; Saint-Girons, I.; Phillips, S. E. V. *Nature* **1989**, *341*, 705.
11. Somers, W. S.; Phillips, S. E. V. *Nature* **1992**, *359*, 387.
12. He, Y. Y.; Stockley, P. G.; Gold, L. *J. Mol. Biol.* **1996**, *255*, 55.
13. Phillips, S. E. V.; Manfield, I.; Parsons, I.; Davidson, B. E.; Rafferty, J. B.; Somers, W. S.; Margarita, D.; Cohen, G. N.; Saint-Girons, I.; Stockley, P. G. *Nature* **1989**, *341*, 711.
14. Aberle, A. M.; Reddy, H. R.; Heeb, N. V.; Nambiar, K. P. *Biochem. Biophys. Res. Commun.* **1994**, *200*, 102.
15. Maynard, A. J.; Searle, M. S. *Chem. Commun.* **1997**, 1297.
16. Maynard, A. J.; Sharman, G. J.; Searle, M. S. *J. Am. Chem. Soc.* **1998**, *120*, 1996.
17. Eickhoff, H.; Jung, G.; Rieker, A. *Tetrahedron* **2001**, *57*, 353.
18. Gottesfeld, J. M.; Neely, L.; Trauger, J. W.; Baird, E. E.; Dervan, P. B. *Nature* **1997**, *387*, 202.
19. Mapp, A. K.; Ansari, A. Z.; Ptashne, M.; Dervan, P. B. *Proc. Natl. Acad. Sci. U.S.A.* **2000**, *97*, 3930.
20. Matthews, J. H.; Dinh, T. D.; Tivitmahaisoon, P.; Ziller, J. W.; Van Vranken, D. L. *Chem. Biol.* **2001**, *8*, 1071.
21. Talanian, R. V.; Mcknight, C. J.; Kim, P. S. *Science* **1990**, *249*, 769.
22. Talanian, R. V.; Mcknight, C. J.; Rutkowski, R.; Kim, P. S. *Biochemistry* **1992**, *31*, 6871. Circular dichroism experiments suggest that specific binding involves only 15 residues, corresponding to residues 231–245 of GCN4, in an alpha-helical conformation. These results limit substantially the region of GCN4 involved in sequence-specific DNA contacts and provide a uniquely simple model for studying protein–DNA interactions in detail.
23. Lajmi, A. R.; Lovrencic, M. E.; Wallace, T. R.; Thomlinson, R. R.; Shin, J. A. *J. Am. Chem. Soc.* **2000**, *122*, 5638.
24. Wadhwa, M. S.; Collard, W. T.; Adami, R. C.; McKenzie, D. L.; Rice, K. G. *Bioconj. Chem.* **1997**, *8*, 81.
25. Helene, C.; Maurizot, J. C. *Crc Crit. Rev. Biochem.* **1981**, *10*, 213.
26. Ollins, D. E.; Ollins, A. L.; von Hippel, P. H. *J. Mol. Biol.* **1968**, *33*, 265.
27. Walse, B.; Kihlberg, J.; Karlsson, K. F.; Nilsson, M.; Wahlund, K. G.; Pinkner, J. S.; Hultgren, S. J.; Drakenberg, T. *FEBS Lett.* **1997**, *412*, 115.
28. Bogusky, M. J.; Culberson, J. C.; Pitzenberger, S. M.; Garsky, V. M.; Wallace, A.; Pessi, A.; Koblan, K. S. *J. Pept. Res.* **1999**, *54*, 66.
29. Seelig, G. F.; Prosise, W. W.; Hawkins, J. C.; Senior, M. M. *J. Biol. Chem.* **1995**, *270*, 9241.
30. Parsons, I. D.; Persson, B.; Mekhalfia, A.; Blackburn, G. M.; Stockley, P. G. *Nucleic Acids Res.* **1995**, *23*, 211.
31. Stockley, P. G.; Baron, A. J.; Wild, C. M.; Parsons, I. D.; Miller, C. M.; Holtham, C. A. M.; Baumberg, S. *Biosensors. Bioelect.* **1998**, *13*, 637.